Pair Density Wave in the Doped *t-J* Model with Ring Exchange on a Triangular Lattice

Xiao Yan Xu,[1,*] K. T. Law,[1,†] and Patrick A. Lee[2,‡]
[1]Department of Physics, Hong Kong University of Science and Technology, Clear Water Bay, Hong Kong, China
[2]Department of Physics, Massachusetts Institute of Technology, Cambridge, Massachusetts 02139, USA

(Received 25 November 2018; published 26 April 2019)

In our previous work [Phys. Rev. Lett. **121**, 046401 (2018)], we found a quantum spin liquid phase with a spinon Fermi surface in the two dimensional spin-1/2 Heisenberg model with four-spin ring exchange on a triangular lattice. In this work we dope the spinon Fermi surface phase by studying the *t-J* model with four-spin ring exchange. We perform density matrix renormalization group calculations on four-leg cylinders of a triangular lattice and find that the dominant pair correlation function is that of a pair density wave; i.e., it is oscillatory while decaying with distance with a power law. The doping dependence of the period is studied. This is the first example where a pair density wave is the dominant pairing in a generic strongly interacting system where the pair density wave cannot be explained as a composite order and no special symmetry is required.

DOI: 10.1103/PhysRevLett.122.167001

A pair density wave (PDW) is a superconducting state in which Cooper pairs have finite momentum. The first example of a PDW is the Fulde-Ferrell-Larkin-Ovchinnikov state [1,2] which can arise in superconductors in strong magnetic fields when the Fermi surface is split by the Zeeman effect. Recently, a PDW has come into prominence in the context of underdoped cuprate superconductors. The striped PDW was proposed as a mechanism for dynamically interlayer decoupling observed in 1/8 hole doped $La_{2-x}Ba_xCuO_4$ [3–6]. One of us has proposed fluctuating bidirectional PDW as the "mother state" that is responsible for many of the anomalous properties of the pseudogap regime [7]. Experimentally, a direct observation of a PDW has been made via local Cooper pair tunneling in $Bi_2Sr_2CaCu_2O_{8+x}$ [8]. They found Cooper pair density modulation with period $4a_0$ where a_0 is the length of unit cell, and the magnitude of the modulation is five percent of the uniform pairing background. This may be interpreted as a subsidiary PDW being generated by the period $4a_0$ charge order together with the uniform *d*-wave pairing. In this sense the recent report [9] of short range period $8a_0$ charge order in the vicinity of the vortex core is even more exciting, because it may be the signature of a hidden period $8a_0$ PDW [10,11].

Theoretically, there are very few microscopic models which are shown to have PDW ground states. Berg *et al.* [12] studied a Kondo-Heisenberg model with 1D electron gas coupled to a spin chain. They found a spin gapped phase with PDW correlations oscillating with period $2a_0$, which matches the period of the ordering tendency of the spin chain. An extended two-leg Hubbard-Heisenberg model is also found to have a spin gapped phase with a PDW [13]. In all these examples, the PDW is commensurate and can either be interpreted as a composite order between short range spin order with the same commensurate period and another short range triplet pairing order, or requires the specially tuned symmetry of π flux through the ladder plaquette. Dodaro *et al.* [14] searched for a PDW in a more standard *t-J* model for doped cuprates, but they did not find any evidence of PDW ordering even when they included next nearest neighbor (NNN) hopping and NNN exchange coupling. On a more speculative level, another mechanism to generate a PDW is the Amperean pairing [7,15], which was first proposed for quantum spin liquids with a spinon Fermi surface. The Ampere effect of the gauge magnetic field produces attractive interactions between spinons moving in the same directions, which creates a PDW with momentum $2k_F$ at a given point on the Fermi surface. In the slave boson theory, the electron operator c_σ is written as $b^\dagger f_\sigma$ where f_σ represents the spinon. Upon doping, the boson b acquires an expectation value in mean field theory, and spinon pairing immediately leads to electron pairing, in this case at finite momentum. This line of reasoning is partly what motivated us to search for a PDW in the context of a doped spin liquid.

Recently, we found the spinon Fermi surface phase in a two dimensional spin-1/2 Heisenberg model with four-spin ring exchange on a triangular lattice [16] using the density matrix renormalization group (DMRG) method. The model is introduced as a microscopic model for Mott insulator phase of 1*T*-TaS_2. The spinon Fermi surface phase was also proposed in early works for organic compounds [17,18] and confirmed in the two-leg and four-leg ladder DMRG simulations [19,20]. We noticed a curious absence of spin structure factor peak along the Γ to M direction and speculated on the possibility of Amperean pairing between the spinons [16]. It is then natural to extend this work to the doped case to see if any evidence of superconductivity

emerges. Based on DMRG calculations on four-leg ladders, we find that upon doping the spinon Fermi surface state, the dominant pairing channel has oscillatory correlations, with a period which depends smoothly on doping and therefore appears to be incommensurate. Also generically the period does not match that of any other charge or spin order, implying that there is no simple interpretation of the PDW as a composite order. The PDW phase we found is very unique and to the best of our knowledge it is the *first* example of a PDW found in a generic interaction driven one band model. This is the key finding in this work.

Model and method.—We consider a t-J model with four-spin ring exchange terms on a triangular lattice, $H = \hat{\mathcal{P}}(H_{t\text{-}J} + H_K)\hat{\mathcal{P}}$, where $\hat{\mathcal{P}}$ excludes doubly occupied states. The hopping and two-spin exchange term $H_{t\text{-}J}$ and four-spin ring exchange term H_K are written as

$$H_{t\text{-}J} = -t\sum_{\langle i,j\rangle\sigma}(c^{\dagger}_{i\sigma}c_{j\sigma} + \text{H.c.}) + J\sum_{\langle i,j\rangle}\mathbf{S}_i\cdot\mathbf{S}_j, \tag{1}$$

$$H_K = K\sum_{\langle i,j,k,l\rangle}[(\mathbf{S}_i\cdot\mathbf{S}_j)(\mathbf{S}_k\cdot\mathbf{S}_l) + (\mathbf{S}_j\cdot\mathbf{S}_k)(\mathbf{S}_i\cdot\mathbf{S}_l) - (\mathbf{S}_i\cdot\mathbf{S}_k)(\mathbf{S}_j\cdot\mathbf{S}_l)], \tag{2}$$

where $\langle i,j\rangle$ denotes the nearest neighbor bond, and $\langle i,j,k,l\rangle$ runs over all compact rhombuses. The ring exchange terms simulate the proximity of the undoped insulator to the Mott transition. We already know from our earlier work on six-leg and eight-leg ladder DMRG simulations that the undoped system enters the spinon Fermi surface phase for $K/J > 0.3$. Here, we investigate the effect of hole doping.

Soon after the discovery of high T_c cuprates, Anderson [21] proposed that doping a Mott insulator may lead to a correlation driven superconductor. Since that time, many methods including mean field theory, Gutzwiller variational methods, and DMRG simulations and exact diagonalization have found d-wave type superconductivity both on square and triangular lattice in some parameter region and doping level [22–26]. We confirm that for the standard t-J model ($K = 0$), doping of the Néel ordered state produces uniform d-wave pair correlations (see Supplemental Material [27]). However, the situation changes completely when we dope into the spinon Fermi surface state. We choose $K/J = 0.8$, which put us quite deep into the spinon Fermi surface phase and $t/J = 2$ which is a conventional value in Mott insulator materials. We perform large-scale DMRG calculations on four-leg ladders with long direction length L_x up to 72. We take periodic boundary conditions in the short direction of the ladder, and open boundary conditions in the long direction. The good quantum numbers of total spin S^z_{tot} and the total number of fermions N_{tot} are used. All the calculations are performed in the $S^z_{\text{tot}} = 0$ and $N_{\text{tot}} = N(1-p)$ sector, where N is the total number of sites and p is the doping level. The calculations are performed with bond dimensions up to $m = 5120$ and the corresponding truncation error is less than 10^{-5}. All the results shown in the following are after extrapolating to an infinite bond dimension if it is not specified. More details are presented in the Supplemental Material [27].

Results.—To study the pairing properties, we measured the pairing correlation in real space. We considered both spin singlet and triplet pairing, and find the magnitude of singlet pairing is always larger than the triplet one, so in the following we will focus on singlet pairing data. The singlet pairing order parameter is defined on nearest neighbor bonds $\Delta_a(i) = c_{i,\uparrow}c_{i+\delta_a,\downarrow} - c_{i,\downarrow}c_{i+\delta_a,\uparrow}$, where δ_a with $a = 1, 2$ takes the value of primitive vectors $\mathbf{a}_1$ and $\mathbf{a}_2$, respectively, denoting different orientation of pairs as shown in the inset of Fig. 1(a). To reduce finite size effects,

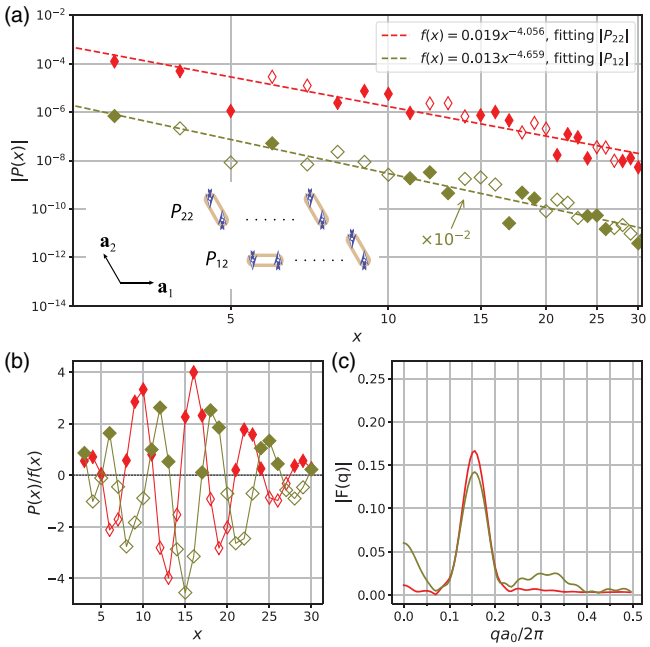

FIG. 1. Pairing correlation along the long direction of the ladder for 1/16 hole doping with $K/J = 0.8$, $t/J = 2$ and four-leg ladder length $L_x = 72$. (a) Log-log plot of the pairing correlation P_{22} and P_{12}. Here, P_{22} is the correlation between pairing order parameters defined both in $\mathbf{a}_2$ orientation, P_{12} is the correlation between pairing order parameters defined in $\mathbf{a}_1$ and $\mathbf{a}_2$ orientation, as showed in the inset. The red thin diamond is for P_{22}, olive diamond is for P_{12}, and the data for P_{12} have been shifted vertically for clarity. The solid symbol is for positive value, while the open symbol is for negative value and we only plot the magnitude. The power law function $f(x)$ in the plot is a fit through the magnitude of the data points. (b) Pairing correlation P_{22} and P_{12} normalized by the power law function $f(x)$, which directly reflects the oscillation of the pairing correlation. The out of phase oscillation of P_{22} and P_{12} indicates a d-wave type pairing. (c) Fourier transform of $P_{22}(x)/f(x)$ and $P_{12}(x)/f(x)$. The peak lies at $0.15(2\pi/a_0)$ both for P_{22} and P_{12}, which gives the total momentum of the pairing.

we measure the correlation functions with a summation over the short direction $P_{aa'}(i_x - i_{x_0}) = \sum_{i_y} \langle \Delta_a^\dagger(i_{x_0}, i_y) \times \Delta_{a'}(i_x, i_y) \rangle$, where (i_x, i_y) is the coordinate of site i in the unit of primitive vectors, i_{x_0} is a reference coordinate in the long direction, we take $i_{x_0} > (L_x/4)$ to reduce the boundary effect, and the final results are averaged over several i_{x_0} s. We denote the relative distance in the correlator by $x = i_x - i_{x_0}$. Figure 1 shows the pairing correlation at doping $1/16$ for both P_{22} and P_{12}. P_{11} is also calculated, but it is very small and is not shown. The pairing correlation shows a clear oscillation with an amplitude which is consistent with a power law decay over a large range of x. (We attribute the deviation from a power law for large x to finite size effect and a lack of convergence.) In the figure, the fit is made to the amplitude of the individual data points which tend to overestimate the exponent of the power law decay. For an oscillatory function, the proper way to fit the exponent requires first extracting the envelop function which we have not attempted here. The purpose of the fit we did is to allow us to display the oscillations on a linear scale, as is done in Fig. 1(b). While the value of the exponent from the fit should not be taken seriously, it is apparently larger than 2, which means that the Fourier transform of the response function will not show divergence for small q and ω. For larger doping of $1/12$ and $1/8$, we also see similar oscillation behavior, but with faster decay and a shorter period with increasing doping (see Fig. 2). The periods are about $7a_0$, $6a_0$, and $4a_0$ for $1/16$, $1/12$, $1/8$ doping, respectively.

In order to identify the pairing symmetry, we analyze the relative phase of P_{22} and P_{12}. It is clear from Fig. 1(b) that P_{22} and P_{12} have out of phase oscillation. Thus, we conclude that we have found a d-wave type PDW.

In addition to the power law decay of the pairing correlation, we also found power law decay of both spin and dimer correlation, corresponding to gapless spin and charge degrees of freedom. In Fig. 3, we show the log-log plot of those correlations. The spin correlations are defined as $S(i_x - i_{x_0}) = \sum_{i_y} \langle \mathbf{S}_{(i_{x_0}, i_y)} \cdot \mathbf{S}_{(i_x, i_y)} \rangle$ and dimer correlations

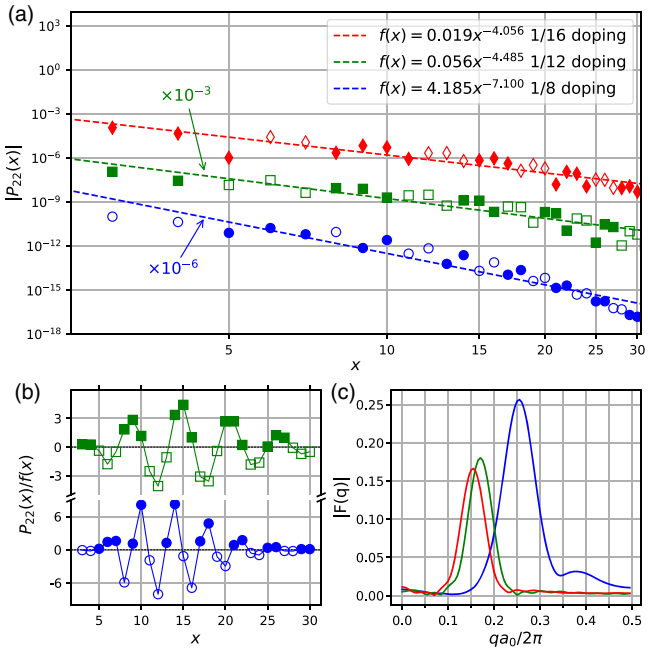

FIG. 2. Pairing correlation P_{22} for different hole doping, $1/16$, $1/12$, and $1/8$, with parameters $K/J = 0.8$, $t/J = 2$, and four-leg ladder length $L_x = 72$. (a) Power law fitting of the magnitude of pairing correlation P_{22} for each doping. The data for $1/12$ and $1/8$ hole doping have been shifted vertically for clarity. (b) Normalized pairing correlation which shows the oscillation part of P_{22} for doping $1/12$ and $1/8$, while $1/16$ doping is already showed in Fig. 1(b). (c) Fourier transformation of the oscillation part of P_{22} for each doping, which gives pairing momentum about $0.15(2\pi/a_0)$, $0.17(2\pi/a_0)$, and $0.25(2\pi/a_0)$ for $1/16$, $1/12$, and $1/8$ hole doping, respectively.

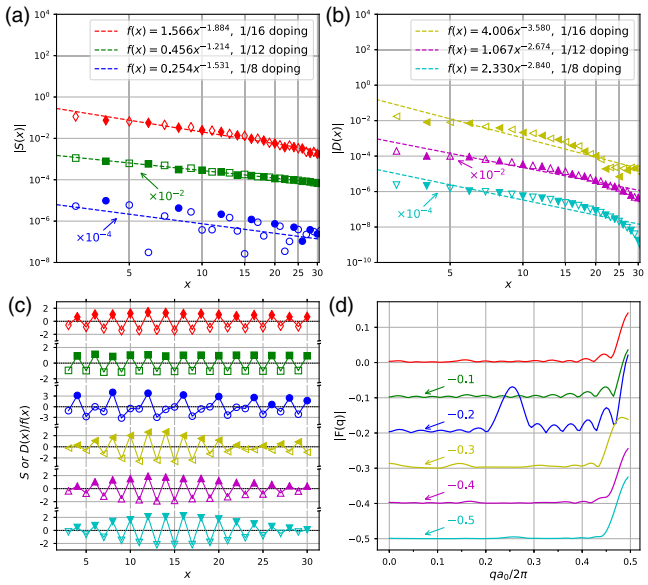

FIG. 3. Spin correlation S and dimer correlation D for different hole doping, $1/16$, $1/12$, and $1/8$, with parameters $K/J = 0.8$, $t/J = 2$, and four-leg ladder length $L_x = 72$. (a) Spin correlation S. Red thin diamond, green square, and blue circle are for $1/16$, $1/12$, and $1/8$ hole doping, respectively. Solid symbol is for positive value, open symbol is for negative value. The magnitude is plotted, and the data points are fitted with a power law. Note the vertical shift of the data for different doping for clarity. (b) Same as (a) for dimer correlation D. Yellow left triangular, magenta up and cyan down are for $1/16$, $1/12$, and $1/8$ hole doping, respectively. Solid symbol is for positive value, open symbol is for negative value. (c) Normalization with the power law function of the magnitude, giving the oscillation part of spin and dimer correlations. (d) Fourier transformation of the oscillatory part of the spin and dimer correlations. The peak gives the ordering momentum; it is $0.25(2\pi/a_0)$ for the spin correlation and $0.5(2\pi/a_0)$ for the dimer correlation at $1/8$ hole doping. For $1/12$ and $1/16$ hole doping it is $0.5(2\pi/a_0)$ for both correlations.

are defined as $D(i_x - i_{x_0}) = \sum_{i_y}(\langle d(i_{x_0}, i_y) d(i_x, i_y)\rangle - \langle d(i_{x_0}, i_y)\rangle\langle d(i_x, i_y)\rangle)$ with $d(i_x, i_y) = \mathbf{S}_{(i_x,i_y)} \cdot \mathbf{S}_{(i_x+1,i_y)}$ the long direction dimer operator. The spin and dimer correlations show slower power law decay compared with the PDW and also show oscillations, and we also analyze their period by Fourier transformation. We find period $2a_0$ for both spin and dimer at hole doping $1/12$ and $1/16$, while at doping $1/8$, we have period $2a_0$ for dimer but period $4a_0$ for spin.

We also measured the Fermi vectors $\mathbf{k}_F$s, which can be estimated by the singular positions of the density in momentum space $n(\mathbf{k})$. The momentum space Fermi density is calculated as $n(\mathbf{k}) = (1/N)\sum_{ij\sigma} e^{i\mathbf{k}\cdot(\mathbf{r}_i - \mathbf{r}_j)}\langle c^\dagger_{i\sigma} c_{j\sigma}\rangle$. Figure 4 shows $n(\mathbf{k})$ along different cuts of the Brillouin zone (BZ). We collect all the singular points in $n(\mathbf{k})$ where the first derivative $\partial n(\mathbf{k})/\partial k_1$ has a dip or peak and get the $\mathbf{k}_F$s shown in the caption of Fig. 4. Although those estimations of $\mathbf{k}_F$ are rather crude, we can make a consistent check of the Fermi surface area based on these $\mathbf{k}_F$s. For example, for $1/8$ hole doping, we add up the distances between the Fermi crossings along the three lines given by $(0, \pm\frac{1}{4})\mathbf{b}_2$ and multiply by the width of each line which is $1/4$ (in the unit of width of the first BZ) to get a total area of $11/24 = 0.4583$ (in the unit of area of the first BZ). This is close to the free fermion value of $(1\text{-}p/2 = 0.4375)$ for the 2D Fermi surface. If we focus on the change of Fermi surface area from $1/8$ to $1/12$ hole doping, we find $1/48$ from this estimate, in precise agreement with what is expected for free Fermions. Thus, we conclude that our interacting quasi-1D system retains the Fermi surface structure expected for Luttinger liquids.

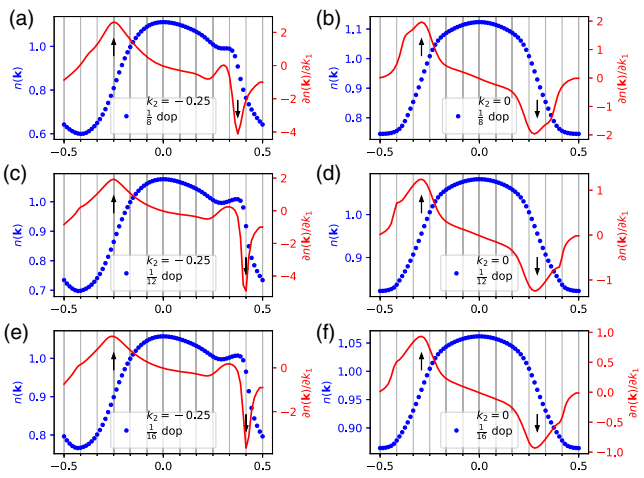

FIG. 4. Momentum space density $n(\mathbf{k})$ and its first derivative in the k_1 direction $\partial n(\mathbf{k})/\partial k_1$, with parameters $K/J = 0.8$, $t/J = 2$, and four-leg ladder length $L_x = 72$. In the plot, k_1 and k_2 are the coordinates of $\mathbf{k}$ points in the unit of primitive vectors in reciprocal space $\mathbf{k} = k_1\mathbf{b}_1 + k_2\mathbf{b}_2$. As there is inversion symmetry, only two cuts $k_2 = -0.25$ and $k_1 = 0$ are shown. The peak and dip positions (denoted by black arrows) of $\partial n(\mathbf{k})/\partial k_1$ give the $\mathbf{k}_F$s. We have $\mathbf{k}_F = \pm\frac{7}{24}\mathbf{b}_1$, $(\frac{3}{8}\mathbf{b}_1 - \frac{1}{4}\mathbf{b}_2)$ and $(-\frac{1}{4}\mathbf{b}_1 - \frac{1}{4}\mathbf{b}_2)$ for $1/8$ hole doping [(a),(b)], $\mathbf{k}_F = \pm\frac{7}{24}\mathbf{b}_1$, $(\frac{5}{12}\mathbf{b}_1 - \frac{1}{4}\mathbf{b}_2)$, and $(-\frac{1}{4}\mathbf{b}_1 - \frac{1}{4}\mathbf{b}_2)$ for $1/12$ [(c),(d)] and $1/16$ hole doping [(e),(f)]. The precision of these values is limited by the finite system size.

The three crossings of Fermi surface from the measurements of $n(\mathbf{k})$ correspond to six gapless modes. To verify it, we measured the subsystem entanglement entropy and fit the central charge with formula $S(l, N) = (c/6)\log[(N/\pi)\sin(\pi l/N)] + A$, where l is the length of the subsystem, N is the total number of sites, c is the central charge, A is a constant, and the $l = 1$ entropy gives a very good estimation of it when N is sufficiently large. While we have not reached convergence, we find that the central charge is at least 4 and is consistent with the central charge of $c = 6$ which supports six gapless modes due to three crossings. The details of the estimations are presented in the Supplemental Material [27].

Discussions.—As the period of spin correlation in $1/8$ hole doping is two times the period of charge correlation and equals the period of a PDW, this is reminiscent of the "antiphase" stripe found in La-based cuprates near $1/8$ hole doping, where the onset of pairing correlations coincides with the onset of static spin-stripe order, and they share the same periodicity [6]. On the other hand, for doping of $1/12$ and $1/16$, there is no such relation between the various periodicity and the PDW cannot be interpreted as stripes. While we do not have a clear picture of what controls the PDW period, we find that the empirical relation for the wave vector, $4\pi p/a_0$, works perfectly for $p = 1/8$ and $1/12$ and within errors for $p = 1/16$. This reminds us of the discussion of pairing of electrons on the same side of the Fermi surface to form a PDW with wave vector $2k_F$ in a one dimensional Luttinger liquid, which was referred to as η pairing [28]. The power law decay is governed by the exponent $\kappa_\rho + 1/\kappa_\rho$ which is always greater than 2 for any value of the Luttinger parameter κ_ρ [28]. If we regard our quasi-1D system as a set of four interacting 1D Luttinger liquids, the quantity that is fixed is the sum of the $2k_F$ from the Fermi crossing of each band and it is given by $4[(1-p)/2](2\pi/a_0)$ where the factor 4 accounts for the fractional BZ area taken up by each 1D band. It is interesting to note that up to umklapp this is just our empirical formula $4\pi p/a_0$.

We believe that the key reason why we find a PDW upon doping the J-K model of the triangular lattice is that we are doping into a spin liquid. While the spin liquid in the undoped system has Fermi surfaces, we do not know whether it is a $U(1)$ spin liquid which has a full Fermi surface, or a $Z2$ spin liquid with a partially gapped Fermi surface. The latter has spinon pairing and it is natural to expect that doping will immediately lead to a pairing state which may be exotic. We indeed find the emergence of an exotic PDW. We do not believe the introduction of the ring exchange term alone is sufficient. We have added the ring exchange term to the t-J model on a square lattice and the leading pairing correlator remains uniform d wave.

In conclusion, we find it encouraging that a dominant PDW correlation emerges upon doping of a model that supports a spinon Fermi surface state. Since this model may be applicable to $1T$-TaS_2, we continue to encourage experimentalists to dope this material by gating in order not to introduce too much disorder [16]. The existence of a fluctuating PDW in a doped Mott insulator model is also encouraging news for the search of a fluctuating PDW in underdoped cuprates [7].

X. Y. X. is thankful for the discussion with E. M. Stoudenmire and Donna Sheng. The calculations are performed using the ITensor C++library (version 2.1.1). X. Y. X. and K. T. L. are thankful for the support of Hong Kong Research Grant Council through C6026-16W, 16324216 and 16307117. K. T. L. is further supported by the Croucher Foundation and the Dr. Tai-chin Lo Foundation. P. A. L. acknowledges support by the U.S. Department of Energy, Basic Energy Sciences under Grant No. DE-FG02-03ER46076. He is thankful for the hospitality of the Institute for Advanced Studies at the Hong Kong University of Science and Technology. The simulation is performed at the Tianhe-2 platform at the National Supercomputer Center in Guangzhou.

*wanderxu@gmail.com
†phlaw@ust.hk
‡palee@mit.edu

[1] P. Fulde and R. A. Ferrell, Superconductivity in a strong spin-exchange field, Phys. Rev. **135**, A550 (1964).
[2] A. I. Larkin and Yu. N. Ovchinnikov, Inhomogeneous state of superconductors, Sov. Phys. JETP **20**, 762 (1965).
[3] A. Himeda, T. Kato, and M. Ogata, Stripe States with Spatially Oscillating d-Wave Superconductivity in the Two-Dimensional $t-t'-J$ Model, Phys. Rev. Lett. **88**, 117001 (2002).
[4] Q. Li, M. Hücker, G. D. Gu, A. M. Tsvelik, and J. M. Tranquada, Two-Dimensional Superconducting Fluctuations in Stripe-Ordered $La_{1.875}Ba_{0.125}CuO_4$, Phys. Rev. Lett. **99**, 067001 (2007).
[5] E. Berg, E. Fradkin, E.-A. Kim, S. A. Kivelson, V. Oganesyan, J. M. Tranquada, and S. C. Zhang, Dynamical Layer Decoupling in a Stripe-Ordered High-T_c Superconductor, Phys. Rev. Lett. **99**, 127003 (2007).
[6] E. Berg, E. Fradkin, S. A. Kivelson, and J. M. Tranquada, Striped superconductors: How spin, charge and superconducting orders intertwine in the cuprates, New J. Phys. **11**, 115004 (2009).
[7] P. A. Lee, Amperean Pairing and the Pseudogap Phase of Cuprate Superconductors, Phys. Rev. X **4**, 031017 (2014).
[8] M. H. Hamidian, S. D. Edkins, S. H. Joo, A. Kostin, H. Eisaki, S. Uchida, M. J. Lawler, E. A. Kim, A. P. Mackenzie, K. Fujita, J. Lee, and J. C. Séamus Davis, Detection of a Cooper-pair density wave in $Bi_2Sr_2CaCu_2O_{8+x}$, Nature (London) **532**, 343 (2016).
[9] S. D. Edkins *et al.*, Magnetic-field induced pair density wave state in the cuprate vortex halo, arXiv:1802.04673.
[10] Y. Wang, S. D. Edkins, M. H. Hamidian, J. C. Séamus Davis, E. Fradkin, and S. A. Kivelson, Pair density waves in superconducting vortex halos, Phys. Rev. B **97**, 174510 (2018).
[11] Z. Dai, Y.-H. Zhang, T. Senthil, and P. A. Lee, Pair-density waves, charge-density waves, and vortices in high-T_c cuprates, Phys. Rev. B **97**, 174511 (2018).
[12] E. Berg, E. Fradkin, and S. A. Kivelson, Pair-Density-Wave Correlations in the Kondo-Heisenberg Model, Phys. Rev. Lett. **105**, 146403 (2010).
[13] A. Jaefari and E. Fradkin, Pair-density-wave superconducting order in two-leg ladders, Phys. Rev. B **85**, 035104 (2012).
[14] J. F. Dodaro, H.-C. Jiang, and S. A. Kivelson, Intertwined order in a frustrated four-leg t-J cylinder, Phys. Rev. B **95**, 155116 (2017).
[15] S.-S. Lee, P. A. Lee, and T. Senthil, Amperean Pairing Instability in the U(1) Spin Liquid State with Fermi Surface and Application to κ-$(BEDT\text{-}TTF)_2Cu_2(CN)_3$, Phys. Rev. Lett. **98**, 067006 (2007).
[16] W.-Y. He, X. Y. Xu, G. Chen, K. T. Law, and P. A. Lee, Spinon Fermi Surface in a Cluster Mott Insulator Model on a Triangular Lattice and Possible Application to $1T$-TaS_2, Phys. Rev. Lett. **121**, 046401 (2018).
[17] O. I. Motrunich, Variational study of triangular lattice spin-1/2 model with ring exchanges and spin liquid state in κ-$(ET)_2cu_2(CN)_3$, Phys. Rev. B **72**, 045105 (2005).
[18] S.-S. Lee and P. A. Lee, U(1) Gauge Theory of the Hubbard Model: Spin Liquid States and Possible Application to κ-$(BEDT\text{-}TTF)_2Cu_2(CN)_3$, Phys. Rev. Lett. **95**, 036403 (2005).
[19] D. N. Sheng, O. I. Motrunich, and M. P. A. Fisher, Spin Bose-metal phase in a spin-$\frac{1}{2}$ model with ring exchange on a two-leg triangular strip, Phys. Rev. B **79**, 205112 (2009).
[20] M. S. Block, D. N. Sheng, O. I. Motrunich, and M. P. A. Fisher, Spin Bose-Metal and Valence Bond Solid Phases in a Spin-1/2 Model with Ring Exchanges on a Four-Leg Triangular Ladder, Phys. Rev. Lett. **106**, 157202 (2011).
[21] P. W. Anderson, The resonating valence bond state in La_2CuO_4 and superconductivity, Science **235**, 1196 (1987).
[22] G. Kotliar and J. Liu, Superexchange mechanism and d-wave superconductivity, Phys. Rev. B **38**, 5142 (1988).
[23] S. R. White and D. J. Scalapino, Ground states of the doped four-leg t-J ladder, Phys. Rev. B **55**, R14701 (1997).
[24] Q.-H. Wang, D.-H. Lee, and P. A. Lee, Doped t-J model on a triangular lattice: Possible application to $Na_xCoO_2 \cdot yH_2O$ and $Na_{1-x}TiO_2$, Phys. Rev. B **69**, 092504 (2004).
[25] H.-C. Jiang, Z.-Y. Weng, and S. A. Kivelson, Superconductivity in the doped t-J model: Results for four-leg cylinders, Phys. Rev. B **98**, 140505(R) (2018).
[26] B.-X. Zheng, C.-M. Chung, P. Corboz, G. Ehlers, M.-P. Qin, R. M. Noack, H. Shi, S. R. White, S. Zhang, and G. K.-L. Chan, Stripe order in the underdoped region of the two-dimensional Hubbard model, Science **358**, 1155 (2017).
[27] See Supplemental Material at http://link.aps.org/supplemental/10.1103/PhysRevLett.122.167001 for details on the DMRG simulation and the results.
[28] V. J. Emery, S. A. Kivelson, and O. Zachar, Classification and stability of phases of the multicomponent one-dimensional electron gas, Phys. Rev. B **59**, 15641 (1999).